ACS OMEGA

http://pubs.acs.org/journal/acsodf

Article

Dendritic Cell Membrane-Derived Nanovesicles for Targeted T Cell Activation

Brock T. Harvey, Xu Fu, Lan Li, Khaga R. Neupane, Namrata Anand, Jill M. Kolesar, and Christopher I. Richards*

Cite This: *ACS Omega* 2022, 7, 46222−46233

Read Online

ACCESS | Metrics & More | Article Recommendations

ABSTRACT: T cells play an integral role in the generation of an effective immune response and are responsible for clearing foreign microbes that have bypassed innate immune system defenses and possess cognate antigens. The immune response can be directed toward a desired target through the selective priming and activation of T cells. Due to their ability to activate a T cell response, dendritic cells and endogenous vesicles from dendritic cells are being developed for cancer immunotherapy treatment. However, current platforms, such as exosomes and synthetic nanoparticles, are limited by their production methods and application constraints. Here, we engineer nanovesicles derived from dendritic cell membranes with similar properties as dendritic cell exosomes via nitrogen cavitation. These cell-derived nanovesicles are capable of activating antigen-specific T cells through direct and indirect mechanisms. Additionally, these nanovesicles can be produced in large yields, overcoming production constraints that limit clinical application of alternative immunomodulatory vesicle or nanoparticle-based methods. Thus, dendritic cell-derived nanovesicles generated by nitrogen cavitation show potential as an immunotherapy platform to stimulate and direct T cell response.

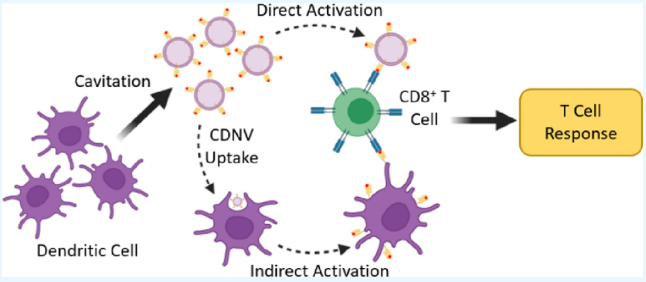

INTRODUCTION

T cells play an integral role in the generation of a sufficient and effective immune response. As a component of the adaptive immune system, T cells work to clear foreign microbes that have bypassed defenses of the innate immune system.[1] Upon activation, CD8$^+$ T cells gain cytotoxic capabilities, eliminating not only cells infected with intracellular microbes, but tumor cells as well.[2] The ability of CD8$^+$ T cells to target and eliminate tumor cells has led to the development of potential therapeutic strategies that harness this capability. While cell-based immunomodulation has shown to be effective to some degree in patients with B cell lymphoma and malignant melanoma, clinical application is limited due to lack of long-term storage stability, risk of in vivo replication and lodging in microvasculature, and susceptibility to immunosuppression.[3−5] An alternative approach is the utilization of extracellular vesicles (EVs) secreted from immune cells that are capable of performing antigen presentation for T cell activation, as they still maintain major histocompatibility complexes (MHCs). For example, exosomes, a subgroup of EVs, possess lipid bilayer membranes that mimic the composition of the parental cell, retaining functional membrane proteins that enable homing to, and interaction with, target cells.[6−12] Exosomes have been found to possess a variety of functional characteristics that have been utilized for therapeutic applications. Such applications include cargo transport between cells, induction of angiogenesis, and immune modulation, rendering them ideal for immunotherapy.[6,13−16]

Exosomes secreted by antigen-presenting cells (APCs), namely, dendritic cells (DC), possess biologically functional MHC surface molecules presenting antigenic peptides (pMHC) capable of inducing antigen-specific T cell responses.[4,13,17−21] When DCs are treated with tumor-associated antigens (TAAs), secreted exosomes retain the ability of parental DC to present these antigens and activate TAA-specific T cells, inducing a TAA-targeted response.[4,5,20,22,23] The function or immunomodulatory ability of exosomes can be further altered or enhanced through surface modification (e.g., amino conjugation, lipid insertion, and PEG (polyethylene glycol)-ylation) or genetic engineering of the parental cell or exosome itself to increase target specificity or load exogenous or endogenous molecules onto the exosome surface or interior.[24,25] Although exosome-based

Received: July 13, 2022
Accepted: November 14, 2022
Published: December 9, 2022

ACS Publications

© 2022 The Authors. Published by American Chemical Society

Scheme 1. Schematic Illustrating Mechanisms of CD8⁺ T Cell Activation Mediated by DC2.4 Cell Membrane-Derived Nanovesicles

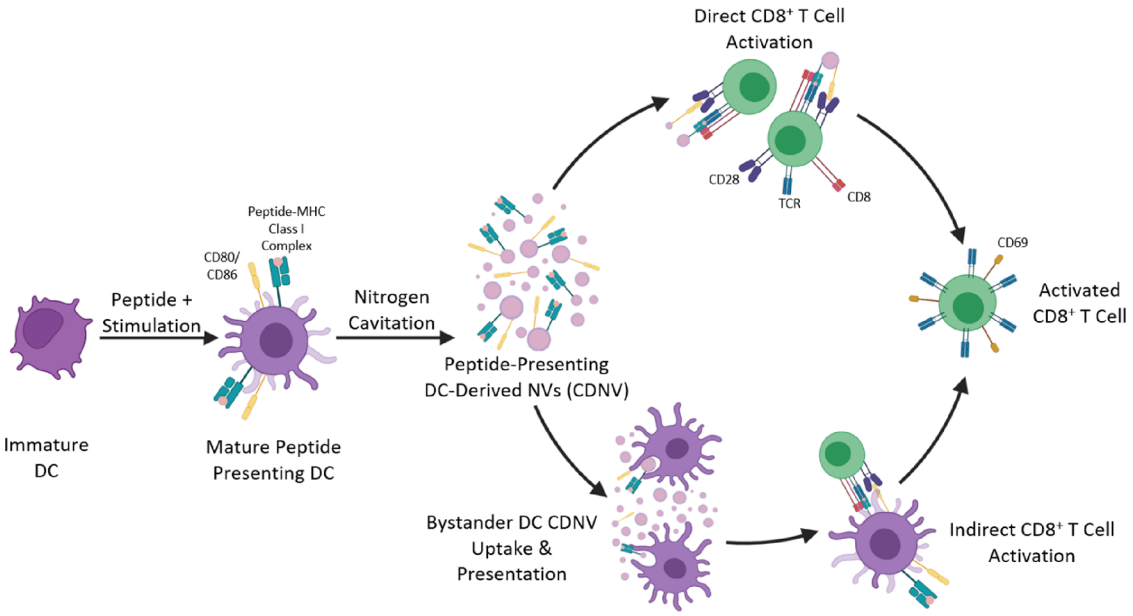

[a]Immature dendritic cells are pulsed with IFN-γ, to stimulate DC2.4 maturation, and antigenic peptide, which is processed and cross-presented in the MHC class I complex. Nitrogen cavitation of mature, peptide-presenting DC2.4 cells generates CDNVs that possess membranes with a similar composition to that of the parental cell and are thus capable of performing many of the same biological functions, such as T cell stimulation. However, CDNVs may participate in direct or indirect CD8⁺ T cell activation. In direct T cell activation (top), CDNVs interact directly with neighboring CD8⁺ T cells and provide activation signals via peptide−MHC (pMHC) class I complexes and costimulatory molecules (CD80/CD86) residing on the CDNV membrane surface with T cell TCR and CD28, respectively. Indirect activation (bottom) is mediated by bystander APCs that take up CDNVs and subsequently process and cross-present antigenic peptide in the cells' own MHC class I complex. Alternatively, APCs may acquire preformed pMHC class I molecules from CDNVs through the transfer of membrane from CDNV to APC in a process termed as cross-dressing. Through these processes, the ability to activate neighboring CD8⁺ T cells may be transferred from CDNV to recipient APC.

cancer immunotherapy has progressed, clinical application is hindered due to manufacturing constraints, such as low yields and a lack of scalable production, giving rise to investigation into alternative, exosome-mimicking platforms.[16,26−30] In an attempt to overcome these obstacles, synthetic alternatives to exosomes have been explored and include systems such as liposomes, dendrimers, nanogels, and metallic nanoparticles. Such systems may possess attributes that enable scalable production, high yields, customizable composition, or modifiable physiochemical properties but are hindered by cost and aggregation during storage and, due to their exogenous nature, lack intrinsic targeting capabilities and can be immunogenic or toxic.[13,16,25,29,31−34] Biomimetic hybrid platforms that employ a synthetic nanoparticle core coated with a cell membrane have been proposed and possess desirable traits, as well as having shown favorable results in mice.[35,36] However, much like exosomes, such platforms are impeded by difficulty in achieving large-scale production, in addition to poor reproducibility and low efficiency in coating the nanoparticle core with cell membrane.[35,37] Cell-derived nanovesicles (CDNVs), which are artificially generated through fragmentation of cell membranes, have shown similar properties as exosomes, including target-specific cargo delivery and the incorporation of peptide-presenting MHC molecules on the CDNV surface to facilitate T cell activation via direct or indirect mechanisms.[38−42] Studies using dendritic cell-derived nanovesicles primarily focused on mediating T cell activation by inducing fusion or aggregation of CDNVs or by simultaneous treatment with CDNVs and free peptides.[38,39] The most commonly used methods of CDNV production rely on ultrasonic or friction/shearing techniques, such as extrusion, that are low throughput, have limited scalability, or denature proteins through generation of high levels of heat.[43,44] Here, we utilize a scalable method of membrane disruption that limits physical damage to generate CDNVs through nitrogen cavitation.[43] We demonstrate the innate ability of DCs to process and present antigenic peptides that can be harnessed and, through cell membrane disruption via nitrogen cavitation, generate high yields of CDNVs from IFN-γ-stimulated DCs capable of driving antigen-specific CD8⁺ T cell activation via both direct and indirect mechanisms under minimal treatment conditions (Figure 1).

METHODS AND MATERIALS

Cell Culture. The hybridoma CD8⁺ T cell line B3Z was generously provided by Dr. J. Woodward (University of Kentucky Medical Center, KY, USA). B3Z cells were cultured in DMEM (Corning) supplemented with 10% heat-inactivated FBS (Corning), 100 unit/mL penicillin, 100 μg/mL streptomycin, 0.292 mg/mL L-glutamine (Gibco), 0.1 mM non-essential amino acids (Gibco), and 1 mM sodium pyruvate (Gibco). The immature dendritic cell line DC2.4 was purchased from Millipore Sigma. DC2.4 cells were cultured in RPMI 1640 medium (Gibco) supplemented with 10% FBS (Corning), 2 mM L-glutamine (Gibco), 0.1 mM non-essential amino acids (Gibco), 10 mM HEPES buffer (Gibco), and 0.5 mM β-mercaptoethanol (Fisher Scientific) for a maximum of 10 passages. Cells were cultured at 37 °C with 5% CO_2.

https://doi.org/10.1021/acsomega.2c04420
ACS Omega 2022, 7, 46222−46233

Nanovesicle Production and Isolation. When indicated, DC2.4 cells were cultured with 20 ng/mL recombinant mouse IFN-γ (Invitrogen) with or without 5 μg/mL SIINFEKL peptide (AnaSpec) overnight. Cells were harvested, washed thoroughly with 1× phosphate-buffered saline (PBS), and then resuspended in protease inhibitor buffer solution, comprised of 1 protease inhibitor tablet (Pierce) per 10 mL 1× PBS, at a concentration of approximately 15×10^6 to 20×10^6 cells/mL. Cell suspension was then transferred to a prechilled cell disruption vessel (Parr Instrument Company, IL, USA) and pressurized to 300 psi under nitrogen for 15 min to achieve pressure equilibration on ice. A pressure of 300 psi was chosen, as nitrogen cavitation at 300 psi has been shown to generate CDNVs within the size range to exosomes.[45] Pressure was released and cell cavitate was collected and centrifuged at 300*g* for 5 min to pellet unfragmented cells. The supernatant was collected, the cell pellet was resuspended in 10 mL of protease inhibitor buffer solution, and nitrogen cavitation was repeated. Cell cavitate was collected, and CDNVs were isolated via differential centrifugation at 500*g* for 10 min, 2000*g* for 20 min, 10,000*g* for 30 min, and 100,000*g* for 90 min, all at 4 °C. Pelleted CDNVs were resuspended in 250−300 μL of 1× PBS and pipetted thoroughly to break up the pellet. Resuspended CDNVs were centrifuged at 7500*g* for 5 min to lightly pellet vesicle aggregates, which were then broken up by additional pipetting. The CDNV suspension was then centrifuged at 7500*g* for 10 min to pellet remaining vesicle aggregates and debris. Proteins, protein aggregates, and free SIINFEKL peptide were removed from nanovesicle suspension by a size-exclusion chromatography PD MiniTrap G-25 column (Cytiva) following the manufacturer's directions. The CDNV suspension was then transferred to a microcentrifuge tube, centrifuged at 10,000*g* for 10 min to remove any remaining debris or aggregates, and then stored at 4 °C until use.

Nanoparticle Tracking Analysis. NTA was performed using a NanoSight NS300 (Malvern) instrument. Samples were measured using fixed camera and detection settings across all sessions. Each sample was recorded for 60 s for a total of five repetitions, with greater than 200 tracks per video, at two dilutions. Analysis was performed using NTA3.4 software.

Western Blot. DC2.4 cells and CDNV pellets were lysed separately in RIPA buffer composed of 150 mM NaCl, 1% Triton X-100, 0.5% sodium deoxycholate, 0.1% SDS, 50 mM Tris (pH 8, adjusted), and 1× protease inhibitor cocktail (Roche). Protein samples were resolved on 12% polyacrylamide gels and then transferred to a nitrocellulose membrane. Equal amounts of protein from various samples were loaded per lane for comparison studies. The nitrocellulose membrane was blocked for 1 h and then incubated with biotinylated anti-mouse CD80 (16-10A1, Biolegend), anti-mouse CD86 (GL-1, Biolegend), or anti-H-2K^b-bound SIINFEKL (25-D1.16, Invivogen) primary antibodies under consistent agitation for 1 h at room temperature in a nonreducing environment. The membrane was then washed and incubated with streptavidin-conjugated HRP (Biolegend) secondary antibody under consistent agitation for 1 h. The membrane was then washed, and bands were visualized by chemiluminescence detection (Clarity, Bio-Rad) using a Chemi-Doc (Bio-Rad) instrument.

Scanning Electron Microscopy. CDNVs were fixed in 2% paraformaldehyde for 45 min and then rinsed with 1× PBS in triplicate. CDNVs were then serially dehydrated in 50, 60, 70, 80, 90, and 100% (200 proof) ethanol for 10 min and resuspended in 200 proof ethanol. Suspended CDNVs were briefly sonicated, and then a droplet of the sample was pipetted and deposited onto silicon wafer. The surface of the sample was then metallized by sputter-coating 5 nm platinum (EM ACE 600, Leica Microsystems, Wetzlar, Germany) to enhance surface electrical conductivity. CDNVs were subsequently imaged using field-emission scanning electron microscopy (feSEM, Helios Nanolab 660, Thermo Fisher Scientific, Hillsboro, OR, USA).

Antibodies and Flow Cytometry. DC2.4 cells were labeled using the following murine monoclonal antibodies from Biolegend, unless stated otherwise: CD16/32 (93), Brilliant Violet 421-conjugated CD11c (N418), phycoerythrin-conjugated CD8α (53-6.7), allophycocyanin-conjugated H-2K^b (AF6-88.5), I-A/I-E (M5/114.15.2), CD40 (1C10, Invitrogen), CD54 (YN1/1.7.4), CD69 (H1.2F3), CD80 (16-10A1), CD86 (GL-1), and H-2K^b-bound SIINFEKL (25-D1.16). Cell viability was determined by staining with Live/Dead Fixable Near-IR Stain (Invitrogen). Isotype-matched antibodies were used as controls. Samples were acquired on a FACSymphony A3 (BD Biosciences) instrument and analyzed with FlowJo (BD).

***In Vitro* T Cell Activation Assay.** To evaluate the ability of CDNVs to activate CD8$^+$ T cells, CNDVs were generated from DC2.4 cells incubated with or without 20 ng/mL IFN-γ and/or 5 μg/mL SIINFEKL peptide overnight. To assess direct T cell activation, CDNVs were added to B3Z cells (3×10^5 cells/well) across a dose range for 18 h with gentle agitation. For indirect T cell activation, CDNVs were added to DC2.4 cells (7.5×10^4 cells/well) across a dose range for 3 h. DC2.4 cells were thoroughly washed and cocultured with B3Z cells (2×10^5 cells/well) for 18 h with gentle agitation. T cell activation was determined by the early T cell activation marker CD69 via flow cytometry.

Bystander APC ELISA Assay. To assess the effect the parental cell maturation status of CDNVs has on bystander APCs, CDNVs were generated from DC2.4 cells incubated with or without 20 ng/mL IFN-γ overnight and added to DC2.4 cells (2×10^5 cells/well) across a dose range for 18 h with gentle agitation. The culture supernatant was collected, and IL-6 was measured by ELISA (MesoScale) following the manufacturer's instructions.

Fluorescence Imaging. DC2.4 cells were plated on 35 mm glass-bottom dishes at 1×10^5 cells/dish and labeled with 2.5 μM DiO (Invitrogen) for 45 min. Resuspended CDNVs were labeled with 5 μM DiI (Invitrogen) for 30 min at 37 °C. Cells were treated with or without 80 μM Dynasore for 30 min prior to CDNV treatment. Cells were treated with 5×10^{10} DiI-labeled CDNVs and incubated for approximately 3 h. Cells were rinsed well and resuspended in L-15 medium (Gibco) for imaging. Cells in 0.4% DMSO (VWR Chemicals) were used as controls.

Statistical Analysis. Statistical analysis was performed using OriginLab 2021b. Flow cytometry data were expressed as the geometric mean ± standard error of the mean (SEM). All other data were expressed as the mean ± SEM. Statistical significance was determined by the two-sample *t*-test or one-way ANOVA with post hoc Tukey's HSD test when appropriate. Statistical significance was indicated as $*p < 0.05$, $**p > 0.01$, and $***p > 0.001$.

■ RESULTS AND DISCUSSION

IFN-γ-Induced DC2.4 Maturation. The importance of DC activation to a mature state is demonstrated by the

https://doi.org/10.1021/acsomega.2c04420
ACS Omega 2022, 7, 46222−46233

increased ability of mature DCs to activate T cells when compared to their immature counterparts.[46−48] To determine the maturation state of the dendritic cell line DC2.4, the cell phenotype was examined for expression of maturation markers by flow cytometry. As shown in Figure 1, unstimulated DC2.4

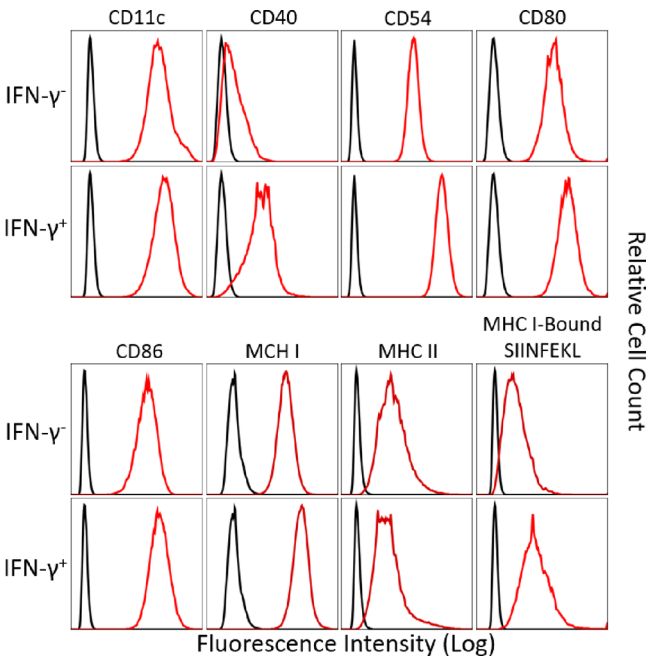

Figure 1. Phenotypic characterization of unstimulated and IFN-γ-stimulated DC2.4 cells. DC2.4 cells were untreated or treated with 20 ng/mL IFN-γ overnight. Expression of CD11c, CD40, CD54, CD80, CD86, MHC class I, MHC class II, and MHC class I-bound SIINFEKL peptide (red) by untreated and IFN-γ treated DC2.4 was analyzed by flow cytometry. Isotype-matched antibodies (black) were used as controls. Following IFN-γ stimulation, DC2.4 expression of the lineage marker CD11c remained constant, and that of maturation markers CD40, CD54, CD80, CD86, and MHC class I increased, while that of the maturation marker MHC class II decreased. Presentation of SIINFEKL peptide by MHC class I also increased following IFN-γ stimulation.

cells were found to have moderate expression of the DC lineage marker CD11c, low expression of the maturation marker CD40, and moderate expression of maturation markers CD54, CD80, CD86, MHC class I, and MHC class II. To activate and induce maturation, DC2.4 cells were cultured with 20 ng/mL IFN-γ overnight. Following incubation with IFN-γ, DC2.4 cells were observed to possess CD11c levels similar to unstimulated cells, while CD40, CD54, CD80, CD86, and MHC class I expression increased, depicted by the increased fluorescence intensity of IFN-γ-treated cells in Figure 1. However, expression of the maturation marker MHC class II unexpectedly decreased. Although MHC class II decreased, the upregulation of maturation markers CD40, CD45, CD80, and CD86 indicates that unstimulated DC2.4 possesses a relative immature phenotype and acquires a mature phenotype following treatment with IFN-γ.

Activation of CD8$^+$ T cells by DCs is MHC class I-restricted, where MHC class I-presented antigenic peptides can be of endogenous or exogenous origin. For example, intracellular infections can result in MHC class I presentation of endogenous peptides, thereby eliciting the targeting of DCs or other cells expressing viral antigens complexed to MHC class I by CD8$^+$ T cells. However, DCs can also direct CD8$^+$ T cells to target other cells, such as tumors, through internalization, processing, and presentation of exogenous antigens, termed as cross-presentation.[2] To evaluate the ability to cross-present exogenous peptides by immature and mature DC2.4, cells were cultured with 5 μg/mL $OVA_{257-264}$ (SIINFEKL) peptide with or without 20 ng/mL IFN-γ and presentation of MHC class I-bound SIINFEKL was measured by flow cytometry. As shown in Figure 1, presentation of MHC class I-bound SIINFEKL increased following IFN-γ stimulation. This demonstrates that the treatment of DC2.4 cells with IFN-γ generates mature DC2.4 cells capable of elevated presentation of exogenous peptide by MHC class I. Thus, due to the increased expression of costimulatory molecules CD80/CD86 and the level of MHC class I-bound SIINFEKL by mature DC2.4 cells, CDNVs generated from mature DC2.4 should mediate CD8$^+$ T cell activation more efficiently than CDNVs from immature DC2.4 cells.

CDNV Characterization. As CD8$^+$ T cell activation is dependent upon the presence of stimulatory pMHC class I and costimulatory molecules CD80 and CD86, retention of these surface proteins on DC2.4-derived CDNVs was verified by western blot (Figure 2). The presence of both costimulatory

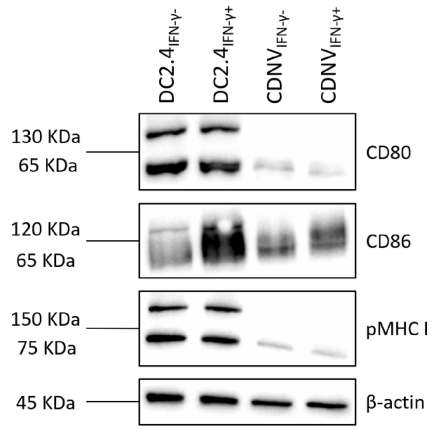

Figure 2. Characterization of CDNV surface proteins by western blot. Western blot of precursor DC2.4 cell and DC2.4-derived CDNVs incubated with 5 μg/mL SIINFEKL peptide and with or without 20 ng/mL IFN-γ overnight. Molecules required for T cell activation, namely, CD80, CD86, and SIINFEKL-presenting MHC class I, were observed on CDNVs from both immature and mature parental DC2.4 cells.

molecules CD80 and CD86, as well as stimulatory MHC class I-bound SIINFEKL, was verified on immature and mature DC2.4, as well as CDNVs generated from immature and mature parental cells. Thus, CDNVs generated from precursor cells by nitrogen cavitation clearly retain the requisite immune-stimulatory molecules for CD8$^+$ T cell activation.

DC maturation is not only associated with changes in protein expression but also morphology.[49,50] To investigate how morphological changes may effect resulting CDNVs or CDNV production, we examined CDNVs from immature and mature DC2.4, generated by nitrogen cavitation and isolated via differential centrifugation. Hereafter, CDNVs generated from unstimulated and IFN-γ-stimulated DC2.4 cells are referred to as immature ($CDNV_{IFN-\gamma^-}$) and mature ($CDNV_{IFN-\gamma^+}$), respectively. As shown in Figure 3A, nanoparticle tracking analysis (NTA) found that both $CDNV_{IFN-\gamma^-}$

https://doi.org/10.1021/acsomega.2c04420
ACS Omega 2022, 7, 46222−46233

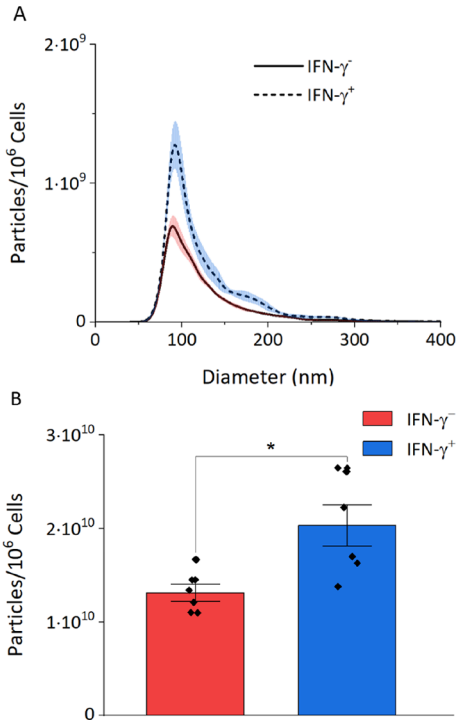

Figure 3. NTA characterization of isolated DC2.4 cell CDNVs following incubation of DC2.4 cells with or without IFN-γ. DC2.4 cells were left untreated or pulsed with 20 ng/mL IFN-γ overnight. Cell membrane-derived nanovesicles were generated by fragmentation of the cell membrane via nitrogen cavitation at 300 psi for 15 min and isolated by differential centrifugation at 500*g*, 2000*g*, 10,000*g*, and 100,000*g*. The CDNV size was measured by nanoparticle tracking analysis (NTA) and NTA3.4 software. (A) Size distribution of CDNVs isolated per 1×10^6 unstimulated (solid line) or IFN-γ-stimulated (dashed line) precursor DC2.4 cells, with average diameters of 123 ± 1 and 125 ± 2 nm, respectively. (B) Total yield of CDNVs per 1×10^6 unstimulated ($1.31 \times 10^{10} \pm 0.9 \times 10^9$) (red) or IFN-$\gamma$-stimulated ($2.0 \times 10^{10} \pm 2 \times 10^9$) (blue) precursor DC2.4 cells (mean ± SEM, $n = 6$). *$p < 0.05$.

and $CDNV_{IFN\text{-}\gamma^+}$ possess a narrow size distribution, with mean diameters of 123 ± 1 and 125 ± 2 nm, respectively. This observed size range is similar to that of endogenous vesicles, such as exosomes. Next, we asked if the precursor cell maturation state effects CDNV yield. While it has previously been demonstrated that immature DCs readily produce exosomes, it has also been shown that DCs treated with LPS, to induce maturation, produce 2- to 3-fold fewer exosomes, on average, than immature DCs.[51] Notably, we found that the yield of CDNVs generated from mature DC2.4 cells increases following IFN-γ stimulation. Following DC2.4 maturation, the CDNV yield increased by approximately 50%, from $1.31 \times 10^{10} \pm 9 \times 10^8$ $CDNV_{IFN\text{-}\gamma^-}$ per 1×10^6 unstimulated precursor cells to $2.0 \times 10^{10} \pm 2 \times 10^9$ $CDNV_{IFN\text{-}\gamma^+}$ per 1×10^6 IFN-γ-stimulated precursor cells (Figure 3B). This increase in CDNV yield following IFN-γ stimulation may be due to morphological changes associated with DC maturation, such as membrane ruffling and formation of dendrites.[49,52] As cell membrane fragmentation by nitrogen cavitation disrupts the cell membrane, which then leads to the formation of small vesicles, these morphological changes may increase the production of CDNVs by increasing the cell membrane surface area available for formation of CDNVs.

CDNVs were further characterized by field-emission scanning electron microscopy (feSEM), as shown in Figure 4A−C. feSEM was found to corroborate the size of nitrogen

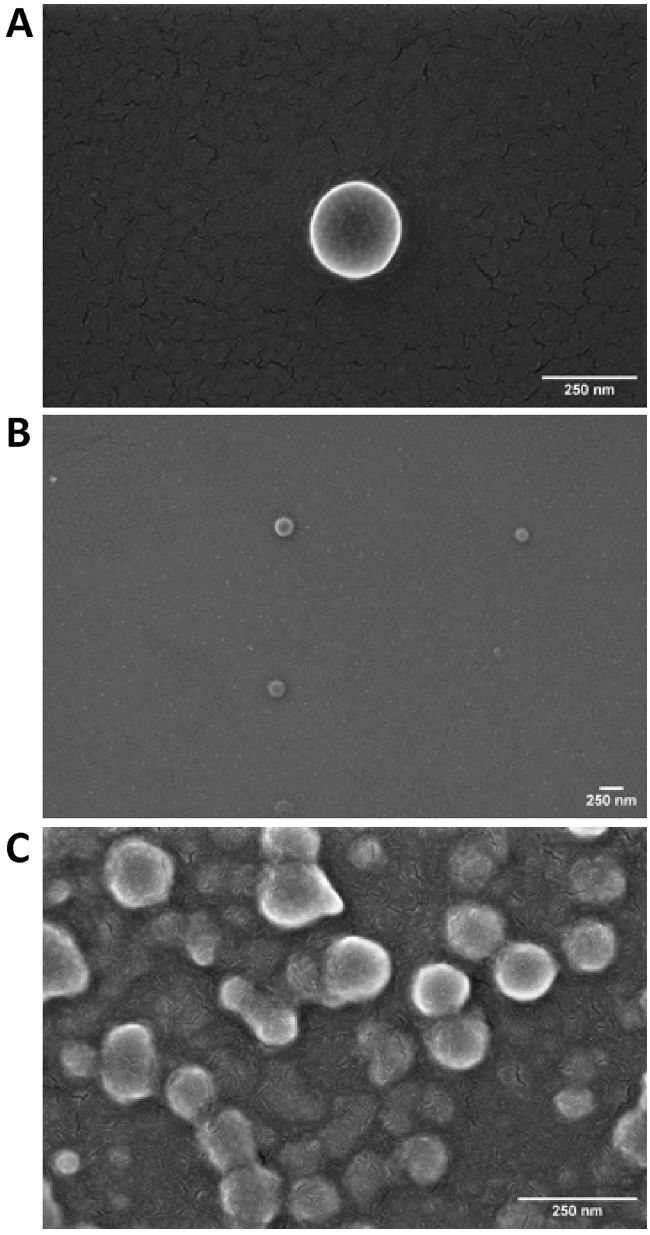

Figure 4. Field-emission scanning electron microscopy images of CDNVs generated from DC2.4 cells. CDNVs generated via nitrogen cavitation and analyzed by feSEM were measured to have a diameter of ∼60−300 nm. CDNV morphology was observed to be highly spherical (A, B) or spherical with some degree of irregularity (**C**). The irregular spherical shape of CDNVs may be a result of sample preparation for feSEM.

cavitation-generated CDNVs measured by NTA, as the diameter of CDNV was measured to range from approximately 60 to 300 nm. The morphology of CDNVs was observed to be mostly spherical, with some irregularity. The irregular spherical shape of CDNVs may be a result of sample preparation, as it has been reported that fixation and dehydration may alter the vesicle shape.[53−55]

Direct CDNV T Cell Activation. Having confirmed the presence of immune-stimulatory molecules on CDNVs by

https://doi.org/10.1021/acsomega.2c04420
ACS Omega 2022, 7, 46222−46233

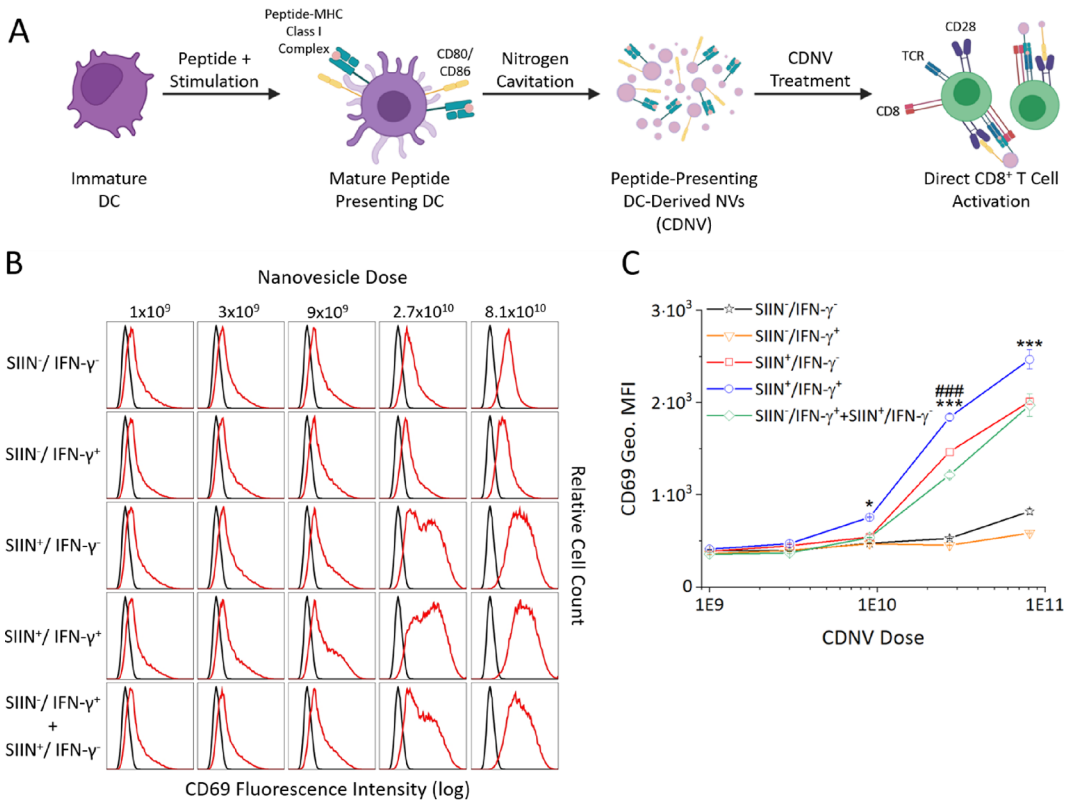

Figure 5. SIINFEKL-presenting CDNVs promote direct activation of T cells. (A) Schematic demonstrating the proposed mechanism of CDNV production and direct activation of T cells. In this approach, immature DC2.4 cells are pulsed with 20 ng/mL IFN-γ to stimulate maturation and 5 μg/mL SIINFEKL peptide for cross-presentation. CDNVs are then generated from mature, peptide-presenting DC2.4 cells by nitrogen cavitation and isolated via differential ultracentrifugation. Direct CD8$^+$ T cell activation is mediated by interaction of pMHC complexes and costimulatory molecules on CDNV$_{SIIN^+/IFN-\gamma^+}$ with TCR and costimulatory receptors on recipient CD8$^+$ T cells. (B) Phenotypic analysis of the T cell early activation marker CD69 following CD8$^+$ T cell treatment with CDNVs generated from immature (IFN-γ^-) or mature (IFN-γ^+) DCs incubated with (SIIN$^+$) or without (SIIN$^-$) SIINFEKL peptide. (C) Expression of CD69, measured as the geometric mean fluorescence intensity (Geo. MFI) following incubation of CDNVs generated from immature (IFN-γ^-) or mature (IFN-γ^+) DCs incubated with (SIIN$^+$) or without (SIIN$^-$) SIINFEKL peptide. Statistical analysis was performed using one-way ANOVA with Tukey's HSD test comparing immature to mature CDNVs (*$p > 0.05$, **$p > 0.01$, and ***$p > 0.001$) or CDNV mixture ($^{\#}p > 0.05$, $^{\#\#}p > 0.01$, and $^{\#\#\#}p > 0.001$) (mean ± SEM, $n = 3$).

western blot (Figure 2), we next investigated the ability of CDNVs generated from DC2.4 cells to stimulate antigen-specific CD8$^+$ T cells via a direct activation mechanism. As shown in Figure 5A, direct activation of T cells by CDNVs involves stimulatory pMHC complexes and costimulatory molecules of the CDNV membrane interacting with the T cell receptor (TCR) and T cell costimulatory receptors, providing signaling that induces T cell activation. Here, CDNVs were generated from DC2.4 cells incubated with or without (CDNV$_{SIIN^+}$ or CDNV$_{SIIN^-}$, respectively) the model peptide SIINFEKL and/or IFN-γ. Isolated CDNVs were incubated with the SIINFEKL-specific, naïve CD8$^+$ T cell line B3Z for 16 h. T cell activation was evaluated by expression of the early activation marker CD69.[56] To determine if CDNVs themselves are capable of activating CD8$^+$ T cells in the absence of SIINFEKL peptide, CDNVs were generated from untreated DC2.4 cells (CDNV$_{SIIN^-/IFN-\gamma^-}$). Upon treatment of CD8$^+$ T cells with CDNV$_{SIIN^-/IFN-\gamma^-}$, the population of CD8$^+$ T cells with low levels of CD69 expression (CD69^{Lo}) (Figure 5B, top row) and geometric mean fluorescence intensity (MFI$_{Geo}$) of T cell CD69 (Figure 5C), representative of the level of T cell activation, was observed to remain constant at doses of 1×10^9 (399 ± 5) and 3×10^9 (393 ± 1) CDNV$_{SIIN^-/IFN-\gamma^-}$. Relatively small increases in CD69 MFI$_{Geo}$ were observed following CD8$^+$ T cell treatment with CDNV$_{SIIN^-/IFN-\gamma^-}$ at doses of 9×10^9 (475 ± 4), 2.7×10^{10} (529 ± 3), and 8.1×10^{10} (820 ± 30). While CD69 MFI$_{Geo}$ trended slightly upward with increasing CDNV$_{SIIN^-/IFN-\gamma^-}$ dose, the change in MFI$_{Geo}$ was not statistically significant. To establish that CD8$^+$ T cell activation is facilitated by stimulatory and costimulatory signals provided by CDNVs, and not directly mediated by a mature CDNV phenotype, DC2.4 cells incubated with only IFN-γ were used to generate mature, non-SIINFEKL-presenting CDNVs (CDNV$_{SIIN^-/IFN-\gamma^+}$). Similar to treatment with CDNV$_{SIIN^-/IFN-\gamma^-}$, the population of CD69^{Lo} (Figure 5B, second row) and CD69 MFI$_{Geo}$ (Figure 5C) of CDNV$_{SIIN^-/IFN-\gamma^+}$-treated CD8$^+$ T cells remained relatively constant, with a slight yet nonsignificant trend upward following treatment with 1×10^9 (361 ± 8), 3×10^9 (400 ± 10), 9×10^9 (470 ± 4), 2.7×10^{10} (454 ± 3), and 8.1×10^{10} (586 ± 6) CDNV$_{SIIN^-/IFN-\gamma^+}$. Little change in the expression of the early activation marker CD69 was observed by treatment with CDNVs from both non-SIINFEKL-presenting immature and mature DC2.4 cells, suggesting that CDNVs lacking antigenic peptide possess relatively low immunogenicity.

With the observation that CDNVs are relatively non-immunogenic in the absence of antigenic peptide, the capability of antigen-presenting CDNVs to stimulate CD8$^+$ T cell activation was investigated by pulsing DC2.4 cells with SIINFEKL peptide with or without IFN-γ. When treated with

https://doi.org/10.1021/acsomega.2c04420
ACS Omega 2022, 7, 46222−46233

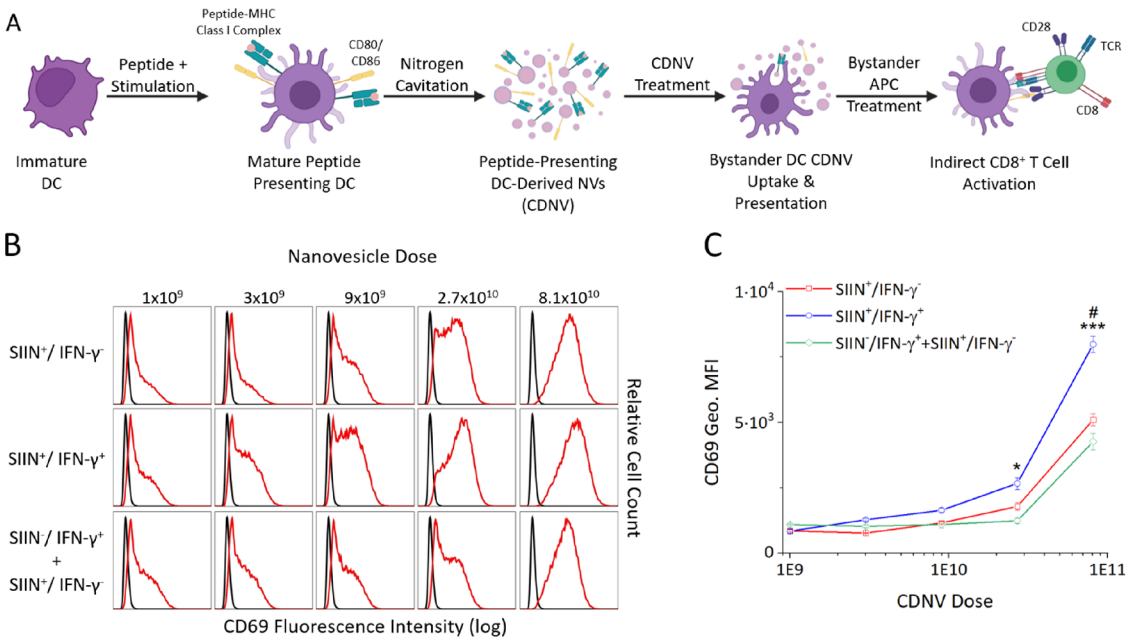

Figure 6. SIINFEKL-presenting CDNVs promote indirect activation of T cells through delivery of antigen to recipient APCs. (A) Schematic demonstrating the mechanism of CDNV production and delivery of antigenic peptide to bystander APCs, conferring the ability to activate T cells. As before, immature DC2.4 cells were pulsed with 20 ng/mL IFN-γ and 5 μg/mL SIINFEKL peptide, which then underwent nitrogen cavitation and differential centrifugation to generate and isolate peptide-presenting CDNVs. Upon DC2.4 treatment with peptide-presenting CDNVs, recipient DC2.4 cells may take up and present antigenic peptides in MHC I complexes on their surface through cross-presentation or cross-dressing. Antigenic peptide-presenting DC2.4 cells then interact with naïve CD8$^+$ T cells, stimulating T cell activation. (B) Phenotypic analysis of T cell activation by T cell early activation marker CD69 expression following CD8$^+$ T cell treatment with DC2.4 cells pulsed with $CDNV_{SIIN^+/IFN\text{-}\gamma^-}$, $CDNV_{SIIN^+/IFN\text{-}\gamma^+}$, or 1:1 mixture of $CDNV_{SIIN^+/IFN\text{-}\gamma^-}$ + $CDNV_{SIIN^+/IFN\text{-}\gamma^+}$ ($CDNV_{Mix}$). (C) Expression of the early T cell activation marker CD69, measured as Geo. MFI, following incubation with DC2.4 cells pulsed with $CDNV_{SIIN^+/IFN\text{-}\gamma^-}$, $CDNV_{SIIN^+/IFN\text{-}\gamma^+}$, or $CDNV_{Mix}$. Statistical analysis was performed using one-way ANOVA with Tukey's HSD test comparing immature to mature CDNVs (*$p > 0.05$, **$p > 0.01$, and ***$p > 0.001$) or CDNV mixture ($^{\#}p > 0.05$, $^{\#\#}p > 0.01$, and $^{\#\#\#}p > 0.001$) (mean ± SEM, $n = 3$).

CDNVs generated from immature, SIINFEKL-presenting DC2.4 ($CDNV_{SIIN^+/IFN\text{-}\gamma^-}$), minimal change in CD69^{Lo} population (Figure 5B, third row) and CD69 MFI_{Geo} (Figure 5C) was observed at the 1×10^9, 3×10^9, and 9×10^9 doses of $CDNV_{SIIN^+/IFN\text{-}\gamma^-}$ (389 ± 9, 450 ± 16, and 540 ± 25, respectively). A significant increase in the population of T cells with elevated CD69 expression (CD69^{Hi}) was observed upon T cell treatment with 2.7×10^{10} $CDNV_{SIIN^+/IFN\text{-}\gamma^-}$ (MFI_{Geo} of 1470 ± 37), eliciting T cell populations of CD69^{Lo} and CD69^{Hi}. Expression of CD69 peaked at the maximum dose of 8.1×10^{10} $CDNV_{SIIN^+/IFN\text{-}\gamma^-}$ (MFI_{Geo} of 2010 ± 32), merging the two T cell populations into a single CD69^{Hi} population, representing activation of the majority of CD8$^+$ T cells.

When treated with mature, SIINFEKL-presenting CDNVs ($CDNV_{SIIN^+/IFN\text{-}\gamma^+}$) produced from IFN-$\gamma$-stimulated, SIINFEKL-pulsed DCs at doses of 1×10^9 and 3×10^9 $CDNV_{SIIN^+/IFN\text{-}\gamma^+}$, CD8$^+$ T cell CD69 expression remained low, with CD69 MFI_{Geo} of 412 ± 1 and 470 ± 12, respectively. The level of T cell activation was observed to progressively increase, indicated by the population shift toward CD69^{Hi} (Figure 5B, fourth row) and an increase in CD69 MFI_{Geo} (Figure 5C), following treatment with 9×10^9 $CDNV_{SIIN^+/IFN\text{-}\gamma^+}$ (MFI_{Geo} of 757 ± 3), with significant increases in T cell activation and CD69 expression upon treatment with 2.7×10^{10} $CDNV_{SIIN^+/IFN\text{-}\gamma^+}$ (MFI_{Geo} of 1840 ± 40) and 8.1×10^{10} $CDNV_{SIIN^+/IFN\text{-}\gamma^+}$ (MFI_{Geo} of 2500 ± 100). Minimal levels of T cell activation occurred after treatment with CDNVs originating from both immature and mature, SIINFEKL-pulsed DC2.4 cells at doses of 1×10^9 and 3×10^9 $CDNV_{SIIN^+/IFN\text{-}\gamma^-}$ or $CDNV_{SIIN^+/IFN\text{-}\gamma^+}$. While the level of T cell activation from treatment with 9×10^9 $CDNV_{SIIN^+/IFN\text{-}\gamma^-}$ remains similar to that observed at lower doses, an increase in T cell activation can be seen at the same dose of 9×10^9 $CDNV_{SIIN^+/IFN\text{-}\gamma^+}$. Similar to results observed during treatment with $CDNV_{SIIN^+/IFN\text{-}\gamma^-}$, treatment with 2.7×10^{10} $CDNV_{SIIN^+/IFN\text{-}\gamma^+}$ yielded a population of both CD69^{Lo} and CD69^{Hi} CD8$^+$ T cells; however, while the population of CD69^{Lo} and CD69^{Hi} appear roughly similar when treated with $CDNV_{SIIN^+/IFN\text{-}\gamma^-}$, the T cell population shifted significantly toward CD69^{Hi} following $CDNV_{SIIN^+/IFN\text{-}\gamma^+}$ treatment. At a dose of 8.1×10^{10} CDNVs, a single CD69^{Hi} T cell population was observed following treatment with both $CDNV_{SIIN^+/IFN\text{-}\gamma^-}$ and $CDNV_{SIIN^+/IFN\text{-}\gamma^+}$, although CD69 MFI_{Geo} levels were higher in $CDNV_{SIIN^+/IFN\text{-}\gamma^+}$-treated samples. We observed the treatment of T cells with 1×10^9 and 3×10^9 $CDNV_{SIIN^+/IFN\text{-}\gamma^+}$ to not be statistically more efficient at T cell activation than that with $CDNV_{SIIN^+/IFN\text{-}\gamma^-}$ at those same doses. However, when treated with 9×10^9, 2.7×10^{10}, or 8.1×10^{10} CDNVs, $CDNV_{SIIN^+/IFN\text{-}\gamma^+}$ was a significantly more potent T cell activator than $CDNV_{SIIN^+/IFN\text{-}\gamma^-}$. As expected, these results support that CDNVs generated from mature, SIINFEKL-presenting DC2.4 are more potent activators of CD8$^+$ T cells than CDNVs from immature, SIINFEKL-presenting DC2.4 cells in direct CD8$^+$ T cell activation.

We further investigated the role of maturation state and subsequent ability of CDNVs to directly activate T cells by examining whether stimulatory and costimulatory signals can be provided by separate CDNVs of different maturation status

https://doi.org/10.1021/acsomega.2c04420
ACS Omega 2022, 7, 46222−46233

or if activation signals need to originate from the same CDNV. $CD8^+$ T cells were incubated with a 1:1 mixture of $CDNV_{SIIN^+/IFN\text{-}\gamma^-}$ + $CDNV_{SIIN^-/IFN\text{-}\gamma^+}$ ($CDNV_{Mix}$). T cells treated with $CDNV_{Mix}$ were observed to have minimal CD69 expression, as determined by CD69 MFI_{Geo}, at doses of 1×10^9 (357 ± 9) and 3×10^9 (371 ± 9), with a small increase upon 9×10^9 (539 ± 4) $CDNV_{Mix}$ treatment. Following treatment with 2.7×10^{10} and 8.1×10^{10} $CDNV_{Mix}$, CD69 expression significantly increased, as CD69 MFI_{Geo} was measured to be 1220 ± 40 and 2000 ± 120, respectively. As shown in Figure 5B,C, T cell activation and CD69 expression mediated by $CDNV_{Mix}$ exhibited a pattern much like that observed in T cells treated with $CDNV_{SIIN^+/IFN\text{-}\gamma^-}$. That is, the relative number of activated T cells and CD69 expression level remained relatively low at doses of 1×10^9, 3×10^9, and 9×10^9, like that observed in $CDNV_{SIIN^+/IFN\text{-}\gamma^-}$-treated samples. Treatment with 2.7×10^{10} $CDNV_{Mix}$ resulted in a population composed primarily of $CD69^{Lo}$ $CD8^+$ T cells, with the emergence of $CD69^{Hi}$ $CD8^+$ T cells, whereas treatment with 8.1×10^{10} $CDNV_{Mix}$ induced a single population comprised primarily of $CD69^{Hi}$ $CD8^+$ T cells. Despite the presence of only half the number of SIINFEKL-presenting CDNVs, $CDNV_{Mix}$ was observed to be similarly efficient at T cell activation as $CDNV_{SIIN^+/IFN\text{-}\gamma^-}$, being statistically less efficient at T cell activation only at the dose of 2.7×10^{10} CDNVs. We interpreted these results as that although costimulatory signals provided by $CDNV_{IFN\text{-}\gamma^-}$ may be reduced relative to $CDNV_{IFN\text{-}\gamma^+}$, mature CDNVs may be able to compensate for this signaling deficit by simultaneous interaction with T cells *in vitro*. However, as facilitation of $CD8^+$ T cell activation by $CDNV_{SIIN^+/IFN\text{-}\gamma^-}$ providing stimulatory signaling with $CDNV_{SIIN^-/IFN\text{-}\gamma^+}$ providing costimulatory signaling requires synchronized interaction with the same cell, such a mechanism of T cell activation may not be significant *in vivo*. Instead, the more likely means of direct T cell activation would occur through stimulatory pMHC and costimulatory signals originating from the same CDNV.

Indirect CDNV T Cell Activation. We have shown that CDNVs are capable of presenting peptides and activating T cells directly. However, CDNV-mediated T cell activation can also occur through indirect means. In contrast to direct activation, indirect activation (Figure 6A) occurs through the uptake of CDNVs by APCs, which, through cross-presentation or cross-dressing, can present antigenic peptides in MHC class I complexes and facilitate $CD8^+$ T cell activation. Previous studies have suggested that *in vivo* exosome-mediated T cell activation is based on the uptake of vesicles in bystander APCs that then travel to lymph nodes, where they present antigenic peptides and activate cognate T cells.[57] Recent studies have also shown that CDNVs can facilitate the delivery of cargo to target cells and alter their immunological function.[42] To assess the ability of CDNVs to deliver peptide and/or functional pMHC complexes and convey T cell stimulatory ability, DC2.4 cells were pretreated with $CDNV_{SIIN^+/IFN\text{-}\gamma^-}$, $CDNV_{SIIN^+/IFN\text{-}\gamma^+}$, or $CDNV_{Mix}$ for 3 h, washed thoroughly, then cocultured with $CD8^+$ T cells. The change in expression of CD69 by the T cell population (Figure 6B) and CD69 MFI_{Geo} (Figure 6C) were then examined. As shown in Figure 6B,C, minimal change in T cell activation was observed by treatment of $CD8^+$ T cells with DC2.4 cells pretreated with 1×10^9 (CD69 MFI_{Geo} of 860 ± 40) or 3×10^9 (CD69 MFI_{Geo} of 768 ± 7) $CDNV_{SIIN^+/IFN\text{-}\gamma^-}$. The population of T cells with elevated CD69 expression marginally increased by treatment with DC2.4 cells pretreated with 9×10^9 $CDNV_{SIIN^+/IFN\text{-}\gamma^-}$ (CD69 MFI_{Geo} of 1160 ± 40), while a significant increase in $CD69^{Hi}$ T cell population by DCs pretreated with 2.7×10^{10} (CD69 MFI_{Geo} of 1800 ± 160) and 8.1×10^{10} (CD69 MFI_{Geo} of 5100 ± 230) $CDNV_{SIIN^+/IFN\text{-}\gamma^-}$ was observed.

When treated with DCs pretreated with $CDNV_{SIIN^+/IFN\text{-}\gamma^+}$ (Figure 6B, middle row), $CD8^+$ T cell activation and CD69 expression were minimal at the lowest dose of 1×10^9 $CDNV_{SIIN^+/IFN\text{-}\gamma^+}$ (MFI_{Geo} of 768 ± 7). The level of T cell activation mediated by DC2.4 cells was observed to progressively increase with increasing dose of $CDNV_{SIIN^+/IFN\text{-}\gamma^+}$ pretreatment. As the $CDNV_{SIIN^+/IFN\text{-}\gamma^+}$ dose increased, CD69 MFI_{Geo} was observed to be 1280 ± 45 at 3×10^9, 1640 ± 80 at 9×10^9, and 2700 ± 230 at 2.7×10^{10} $CDNV_{SIIN^+/IFN\text{-}\gamma^+}$, peaking at 8000 ± 300 upon $CD8^+$ T cell treatment with DC2.4 cells pretreated with 8.1×10^{10} $CDNV_{SIIN^+/IFN\text{-}\gamma^+}$. No statistical difference in T cell activation was observed between $CDNV_{SIIN^+/IFN\text{-}\gamma^-}$ and $CDNV_{SIIN^+/IFN\text{-}\gamma^+}$ at doses of 1×10^9, 3×10^9, and 9×10^9, although T cell CD69 MFI_{Geo} tended to be slighter higher from $CDNV_{SIIN^+/IFN\text{-}\gamma^+}$ at doses 3×10^9 and 9×10^9 CDNVs. However, $CDNV_{SIIN^+/IFN\text{-}\gamma^+}$ was statistically more efficient at concentrations of 2.7×10^{10} and 8.1×10^{10} CDNVs. Expectedly, CDNVs derived from mature, SIINFEKL-presenting DC2.4 cells were observed to be more potent activators of $CD8^+$ T cells than CDNVs derived from their immature counterparts. We also noted that although CDNVs can activate $CD8^+$ T cells through a direct mechanism, indirect activation of T cells through uptake and presentation by bystander DC2.4 cells was far more efficient. Results of DC2.4-mediated indirect activation suggest that $CDNV_{SIIN^+/IFN\text{-}\gamma^+}$ may increase the T cell activation efficiency of recipient DC2.4 cells through two ways: (1) inducing maturation of recipient DCs or (2) increased level of SIINFEKL-MHC class I delivered for cross-presentation or cross-dressing of recipient DCs.

To investigate if the increased efficacy of $CD8^+$ T cell activation by DC2.4 cells incubated with $CDNV_{SIIN^+/IFN\text{-}\gamma^+}$ is the result of the mature phenotype of precursor cells, DC2.4 cells were treated with $CDNV_{Mix}$. When treated with DC2.4 cells pretreated with $CDNV_{Mix}$ (Figure 6B, bottom row) at doses of 1×10^9, 3×10^9, and 9×10^9, $CD8^+$ T cell activation remained relatively low and constant, as CD69 MFI_{Geo} was observed to be 1090 ± 29, 1027 ± 45, and 1094 ± 125, respectively, much like treatment with $CDNV_{SIIN^+/IFN\text{-}\gamma^-}$. The number of $CD8^+$ T cells with elevated CD69 expression slightly rose following treatment with DC2.4 cells pretreated with 2.7×10^{10} (CD69 MFI_{Geo} of 1200 ± 100) $CDNV_{Mix}$, while $CD8^+$ T cell activation significantly increased upon treatment with DC2.4 cells pretreated with 8.1×10^{10} (MFI_{Geo} of 4300 ± 300) $CDNV_{Mix}$.

$CDNV_{SIIN^+/IFN\text{-}\gamma^-}$ was statistically more efficient at indirect T cell activation than $CDNV_{Mix}$, but only at the 8.1×10^{10} CDNV dose. Despite the presence of $CDNV_{SIIN^-/IFN\text{-}\gamma^+}$ to assist in any potential activation of recipient DC2.4 cells, and similar to results observed in the direct activation assay, $CD8^+$ T cell activation by $CDNV_{Mix}$ more closely resembled treatment with $CDNV_{SIIN^+/IFN\text{-}\gamma^-}$ than $CDNV_{SIIN^+/IFN\text{-}\gamma^+}$. Activation of $CD8^+$ T cells by bystander DC2.4 cells was less efficient when DC2.4 cells were treated with $CDNV_{Mix}$, suggesting that $CDNV_{IFN\text{-}\gamma^+}$ may not activate recipient DC2.4 cells, but instead, mature CDNVs may deliver increased SIINFEKL in complex with MHC class I molecules for cross-

https://doi.org/10.1021/acsomega.2c04420
ACS Omega 2022, 7, 46222−46233

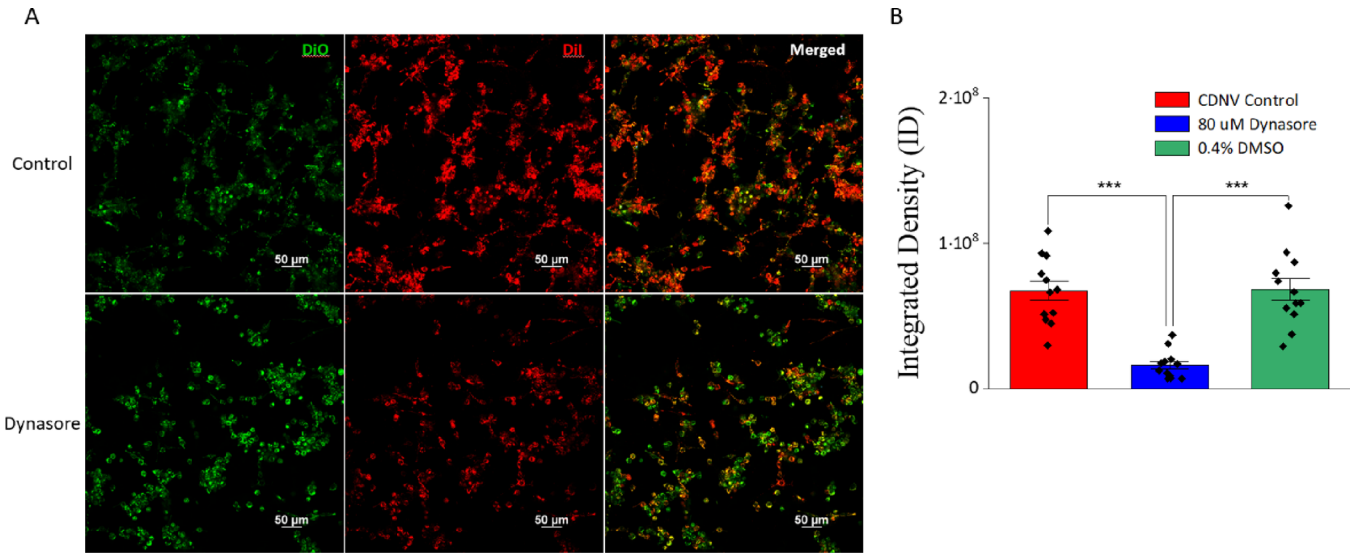

Figure 7. DC2.4 CDNVs are taken up by bystander DC2.4 cells primarily through clathrin-mediated routes. (A) DC2.4 cell membranes were labeled with lipophilic membrane stain DiO (green). CDNVs from DC2.4 cells were labeled with DiI (red). Bystander DiO-labeled DC2.4 cells were pretreated with or without 80 μM clathrin-mediated endocytosis inhibitor Dynasore for 30 min. DiO-labeled DC2.4 cells were then cultured with 5×10^{10} DiI-labeled CDNVs with or without Dynasore for 3 h and imaged by confocal microscopy. Cells in 0.4% DMSO were used as the control. (B) CDNV uptake by bystander APCs was measured by the fluorescence of cellular DiI. The integrated density (ID) was calculated from fluorescence images. Statistical analysis was performed using one-way ANOVA with Tukey's HSD test (***$p > 0.001$) (mean ± SEM, $n = 9$).

presentation or cross-dressing that results in more efficient activation of $CD8^+$ T cells than $CDNV_{SIIN^+/IFN\text{-}\gamma^-}$.

CDNVs and Bystander DCs. To investigate the mechanism of DC−CDNV interaction with bystander DC2.4 cells, DC2.4 cells were labeled with lipophilic fluorescent label DiO and incubated with 5×10^{10} CDNVs, labeled with DiI, for 3 h with or without the clathrin-mediated endocytosis inhibitor Dynasore, which blocks ≥90% of endocytosis at a concentration of 80 μM.[58] Cells in 0.4% DMSO were used as a control. Cells were imaged by confocal microscopy, and DiI-labeled CDNV uptake was calculated using integrated density (ID), i.e., the product of area in pixels and mean gray value. As shown in Figure 7, untreated DC2.4 cells had an ID of $6.7 \times 10^7 \pm 8 \times 10^6$, while the uptake of DiI-labeled CDNVs by DC2.4 in the presence of 80 μM Dynasore significantly decreased, as ID for cells treated with Dynasore was observed to be $1.6 \times 10^7 \pm 3 \times 10^6$. The presence of DMSO was not observed to influence CDNV uptake by DC2.4 cells, as DiI-labeled CNDV uptake by untreated DC2.4 cells was similar to that by DC2.4 cells treated with 0.4% DSMO (ID of $6.8 \times 10^8 \pm 9 \times 10^6$). As CDNV uptake by untreated cells was significantly higher than that by cells treated with Dynasore, the uptake of CDNVs by recipient bystander DC2.4 cells primarily occurs through a clathrin-mediated route.

It has previously been reported that CDNVs generated from macrophages are capable of mediating repolarization between pro- and anti-inflammatory states of recipient macrophage cells.[42] With this in mind, we examined the effect DC2.4 CDNVs have on the activation of recipient DC2.4 cells (Figure 8). To investigate if DC2.4-derived CDNVs are capable of inducing maturation of recipient bystander APCs, DC2.4 cells were treated with CDNVs generated from immature ($CDNV_{IFN\text{-}\gamma^-}$) or IFN-$\gamma$-induced mature ($CDNV_{IFN\text{-}\gamma^+}$) parental cells for 24 h and interleukin-6 (IL-6) production was measured by ELISA. Although a trend of increased IL-6 production with increasing CDNV dose was observed with DC2.4 cells treated with both $CDNV_{IFN\text{-}\gamma^-}$ and $CDNV_{IFN\text{-}\gamma^+}$,

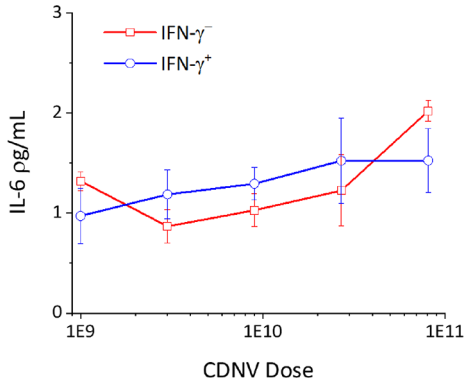

Figure 8. CDNV effect on IL-6 cytokine production of recipient DC2.4 cells. DC2.4 cells were cultured with CDNVs generated from immature DC2.4 ($CDNV_{IFN\text{-}\gamma^-}$) or mature DC2.4 ($CDNV_{IFN\text{-}\gamma^+}$) cells for 18 h, and IL-6 production was measured via ELISA. Statistical analysis was performed using one-way ANOVA with Tukey's HSD test (mean ± SEM, $n = 3$).

IL-6 production did not significantly differ across the dose range or between $CDNV_{IFN\text{-}\gamma^-}$- and $CDNV_{IFN\text{-}\gamma^+}$-treated DC2.4. These results suggest that CDNVs originating from IFN-γ-induced mature DC2.4 cells lack the ability to induce maturation of immature recipient DC2.4 cells.

■ CONCLUSIONS

Due to the limitations of cells in immunotherapy, exosomes and other small extracellular vesicles or synthetic nanoparticles have been proposed and studied as a replacement for cell-based immunotherapy. However, such immunomodulatory platforms are plagued by shortcomings that restrict their application in a clinical setting. Here, we show that the intrinsic ability of DCs to process and present antigens can be harnessed and combined with fragmentation of the cell membrane by nitrogen cavitation to generate cell membrane-derived nanovesicles that retain the cell composition of the

https://doi.org/10.1021/acsomega.2c04420
ACS Omega 2022, 7, 46222−46233

precursor cell membrane. We have shown that these CDNVs possess the capability to present antigens and facilitate activation of antigen-specific $CD8^+$ T cells by both direct interaction with T cells and indirect activation through uptake by bystander DCs that then activate $CD8^+$ T cells. Not only do CDNVs retain the necessary surface molecules required for $CD8^+$ T cell activation, but also CDNVs generated by nitrogen cavitation can be produced in higher yields while being less labor-intensive than exosomes. Furthermore, the production efficiency of CDNVs is enhanced following maturation, increasing the yield of CDNVs with higher T cell activation efficacy in contrast exosomes, which suffer from a decrease in yield following maturation. Thus, DC cell membrane-derived nanovesicles generated by nitrogen cavitation offer a potential platform for immunotherapy to surmount limitations associated with cell-, exosome-, and synthetic nanoparticle-based methods.

AUTHOR INFORMATION

Corresponding Author

Christopher I. Richards − *Department of Chemistry, College of Arts and Sciences, University of Kentucky, Lexington, Kentucky 40506, United States;* orcid.org/0000-0003-0019-1989; Email: chris.richards@uky.edu

Authors

Brock T. Harvey − *Department of Chemistry, College of Arts and Sciences, University of Kentucky, Lexington, Kentucky 40506, United States*

Xu Fu − *Light Microscopy Facility, University of Kentucky, Lexington, Kentucky 40506, United States;* orcid.org/0000-0002-8577-2127

Lan Li − *Department of Chemistry, College of Arts and Sciences, University of Kentucky, Lexington, Kentucky 40506, United States*

Khaga R. Neupane − *Department of Chemistry, College of Arts and Sciences, University of Kentucky, Lexington, Kentucky 40506, United States*

Namrata Anand − *Department of Pharmacy and Practice, College of Pharmacy, University of Kentucky, Lexington, Kentucky 40506, United States*

Jill M. Kolesar − *Department of Pharmacy and Practice, College of Pharmacy, University of Kentucky, Lexington, Kentucky 40506, United States*

Complete contact information is available at: https://pubs.acs.org/10.1021/acsomega.2c04420

Author Contributions

B.T.H. and C.I.R. wrote the manuscript. B.T.H, C.I.R., and J.M.K. designed the experiments. B.T.H., X.F., L.L., K.R.N., and N.A. performed the experiments.

Funding

Support for this work was provided by the Kentucky Pediatric Cancer Research Trust Fund (PON2 728 2000002500).

Notes

The authors declare no competing financial interest.

ACKNOWLEDGMENTS

We thank the Flow Cytometry Shared Resource Facility of the University of Kentucky Markey Cancer Center (P30CA177558) and Light Microscopy Core at the University of Kentucky for flow cytometry and confocal microscopy experiments, respectively. Access to characterization instruments and staff assistance was provided by the Electron Microscopy Center at the University of Kentucky, member of the KY INBR (Kentucky IDeA Networks for Biomedical Research Excellence), which is funded by the National Institute of Health (NIH) National Institute of General Medical Science (IDeA Grant P20GM103436), and of the National Nanotechnology Coordinated Infrastructure (NNCI), which is supported by the National Science Foundation (ECCS-1542164). Illustrations were created with BioRender.com.

REFERENCES

(1) Chaplin, D. D. Overview of the immune response. *J. Allergy Clin. Immunol.* **2010**, *125*, S3−S23.

(2) Gil-Torregrosa, B. C.; Lennon-Duménil, A. M.; Kessler, B.; Guermonprez, P.; Ploegh, H. L.; Fruci, D.; van Endert, P.; Amigorena, S. Control of cross-presentation during dendritic cell maturation. *Eur. J. Immunol.* **2004**, *34*, 398−407.

(3) Brossart, P.; Wirths, S.; Stuhler, G.; Reichardt, V. L.; Kanz, L.; Brugger, W. Induction of cytotoxic T-lymphocyte responses in vivo after vaccinations with peptide-pulsed dendritic cells. *Blood* **2000**, *96*, 3102−3108.

(4) Shenoda, B. B.; Ajit, S. K. Modulation of Immune Responses by Exosomes Derived from Antigen-Presenting Cells. *Clin. Med. Insights: Pathol.* **2016**, *9s1*, 1−8.

(5) Pitt, J. M.; Charrier, M.; Viaud, S.; André, F.; Besse, B.; Chaput, N.; Zitvogel, L. Dendritic Cell−Derived Exosomes as Immunotherapies in the Fight against Cancer. *J. Immunol.* **2014**, *193*, 1006−1011.

(6) Beit-Yannai, E.; Tabak, S.; Stamer, W. D. Physical exosome:exosome interactions. *J. Cell. Mol. Med.* **2018**, *22*, 2001−2006.

(7) Hartjes, T. A.; Mytnyk, S.; Jenster, G. W.; van Steijn, V.; van Royen, M. E. Extracellular Vesicle Quantification and Characterization: Common Methods and Emerging Approaches. *Bioengineering (Basel)* **2019**, *6*, 7.

(8) Tkach, M.; Théry, C. Communication by Extracellular Vesicles: Where We Are and Where We Need to Go. *Cell* **2016**, *164*, 1226−1232.

(9) Mathivanan, S.; Ji, H.; Simpson, R. J. Exosomes: extracellular organelles important in intercellular communication. *J. Proteomics* **2010**, *73*, 1907−1920.

(10) Mulcahy, L. A.; Pink, R. C.; Carter, D. R. F. Routes and mechanisms of extracellular vesicle uptake. *J. Extracell. Vesicles* **2014**, *3*, 24641.

(11) Xia, X.; Wang, Y.; Huang, Y.; Zhang, H.; Lu, H.; Zheng, J. C. Exosomal miRNAs in central nervous system diseases: biomarkers, pathological mediators, protective factors and therapeutic agents. *Prog. Neurobiol.* **2019**, *183*, No. 101694.

(12) El Andaloussi, S.; Lakhal, S.; Mäger, I.; Wood, M. J. A. Exosomes for targeted siRNA delivery across biological barriers. *Adv. Drug Delivery Rev.* **2013**, *65*, 391−397.

(13) Man, K.; Brunet, M. Y.; Jones, M.-C.; Cox, S. C. Engineered Extracellular Vesicles: Tailored-Made Nanomaterials for Medical Applications. *Nanomaterials (Basel)* **2020**, *10*, 1838.

(14) Sun, D.; Zhuang, X.; Zhang, S.; Deng, Z.-B.; Grizzle, W.; Miller, D.; Zhang, H.-G. Exosomes are endogenous nanoparticles that can deliver biological information between cells. *Adv. Drug Delivery Rev.* **2013**, *65*, 342−347.

(15) Morelli, A. E.; Larregina, A. T.; Shufesky, W. J.; Sullivan, M. L.; Stolz, D. B.; Papworth, G. D.; Zahorchak, A. F.; Logar, A. J.; Wang, Z.; Watkins, S. C.; Falo, L. D., Jr.; Thomson, A. W. Endocytosis, intracellular sorting, and processing of exosomes by dendritic cells. *Blood* **2004**, *104*, 3257−3266.

(16) Das, C. K.; Jena, B. C.; Banerjee, I.; Das, S.; Parekh, A.; Bhutia, S. K.; Mandal, M. Exosome as a Novel Shuttle for Delivery of Therapeutics across Biological Barriers. *Mol. Pharmaceutics* **2019**, *16*, 24−40.

(17) Huppa, J. B.; Davis, M. M. T-cell-antigen recognition and the immunological synapse. *Nat. Rev. Immunol.* **2003**, *3*, 973−983.
(18) Théry, C.; Ostrowski, M.; Segura, E. Membrane vesicles as conveyors of immune responses. *Nat. Rev. Immunol.* **2009**, *9*, 581−593.
(19) Greening, D. W.; Gopal, S. K.; Xu, R.; Simpson, R. J.; Chen, W. Exosomes and their roles in immune regulation and cancer. *Semin. Cell Dev. Biol.* **2015**, *40*, 72−81.
(20) Pitt, J. M.; Kroemer, G.; Zitvogel, L. Extracellular vesicles: masters of intercellular communication and potential clinical interventions. *J. Clin. Invest.* **2016**, *126*, 1139−1143.
(21) Chaput, N.; Théry, C. Exosomes: immune properties and potential clinical implementations. *Semin. Immunopathol.* **2011**, *33*, 419−440.
(22) Zitvogel, L.; Regnault, A.; Lozier, A.; Wolfers, J.; Flament, C.; Tenza, D.; Ricciardi-Castagnoli, P.; Raposo, G.; Amigorena, S. Eradication of established murine tumors using a novel cell-free vaccine: dendritic cell derived exosomes. *Nat. Med.* **1998**, *4*, 594−600.
(23) Robbins, P. D.; Morelli, A. E. Regulation of immune responses by extracellular vesicles. *Nat. Rev. Immunol.* **2014**, *14*, 195−208.
(24) Dooley, K.; McConnell, R.; Xu, K.; Lewis, N.; Haupt, S.; Youniss, M.; Martin, S.; Sia, C.; McCoy, C.; Moniz, R.; Burenkova, O.; Sanchez-Salazar, J.; Jang, S. C.; Choi, B.; Harrison, R. A.; Houde, D.; Burzyn, D.; Leng, C.; Kirwin, K.; Ross, N. L.; Finn, J. D.; Gaidukov, L.; Economides, K. D.; Estes, S.; Thornton, J. E.; Kulman, J. D.; Sathyanarayanan, S.; Williams, D. E. A Versatile Platform for Generating Engineered Extracellular Vesicles with Defined Therapeutic Properties. *Mol. Ther.* **2021**, *29*, 1729.
(25) Jafari, D.; Shajari, S.; Jafari, R.; Mardi, N.; Gomari, H.; Ganji, F.; Forouzandeh Moghadam, M.; Samadikuchaksaraei, A. Designer Exosomes: A New Platform for Biotechnology Therapeutics. *BioDrugs* **2020**, *34*, 567−586.
(26) Escudier, B.; Dorval, T.; Chaput, N.; André, F.; Caby, M. P.; Novault, S.; Flament, C.; Leboulaire, C.; Borg, C.; Amigorena, S.; et al. Vaccination of metastatic melanoma patients with autologous dendritic cell (DC) derived-exosomes: results of thefirst phase I clinical trial. *J. Transl. Med.* **2005**, *3*, 10.
(27) Morse, M. A.; Garst, J.; Osada, T.; Khan, S.; Hobeika, A.; Clay, T. M.; Valente, N.; Shreeniwas, R.; Sutton, M. A.; Delcayre, A.; et al. A phase I study of dexosome immunotherapy in patients with advanced non-small cell lung cancer. *J. Transl. Med.* **2005**, *3*, 9.
(28) Besse, B.; Charrier, M.; Lapierre, V.; Dansin, E.; Lantz, O.; Planchard, D.; Le Chevalier, T.; Livartoski, A.; Barlesi, F.; Laplanche, A.; et al. Dendritic cell-derived exosomes as maintenance immunotherapy after first line chemotherapy in NSCLC. *OncoImmunology* **2016**, *5*, No. e1071008.
(29) Soltani, F.; Parhiz, H.; Mokhtarzadeh, A.; Ramezani, M. Synthetic and Biological Vesicular Nano-Carriers Designed for Gene Delivery. *Curr. Pharm. Des.* **2015**, *21*, 6214−6235.
(30) Vader, P.; Mol, E. A.; Pasterkamp, G.; Schiffelers, R. M. Extracellular vesicles for drug delivery. *Adv. Drug Delivery Rev.* **2016**, *106*, 148−156.
(31) Min, Y.; Caster, J. M.; Eblan, M. J.; Wang, A. Z. Clinical Translation of Nanomedicine. *Chem. Rev.* **2015**, *115*, 11147−11190.
(32) Sukhanova, A.; Bozrova, S.; Sokolov, P.; Berestovoy, M.; Karaulov, A.; Nabiev, I. Dependence of Nanoparticle Toxicity on Their Physical and Chemical Properties. *Nanoscale Res. Lett.* **2018**, *13*, 44.
(33) Szebeni, J.; Moghimi, S. M. Liposome triggering of innate immune responses: a perspective on benefits and adverse reactions. *J. Liposome Res.* **2009**, *19*, 85−90.
(34) Xu, C.; Ju, D.; Zhang, X. Cell Membrane-Derived Vesicle: A Novel Vehicle for Cancer Immunotherapy. *Front. Immunol.* **2022**, *13*, No. 923598.
(35) Zeng, Y.; Li, S.; Zhang, S.; Wang, L.; Yuan, H.; Hu, F. Cell membrane coated-nanoparticles for cancer immunotherapy. *Acta Pharm. Sin. B* **2022**, *12*, 3233−3254.
(36) Cheng, S.; Xu, C.; Jin, Y.; Li, Y.; Zhong, C.; Ma, J.; Yang, J.; Zhang, N.; Li, Y.; Wang, C.; et al. Artificial Mini Dendritic Cells Boost T Cell-Based Immunotherapy for Ovarian Cancer. *Adv. Sci. (Weinh)* **2020**, *7*, 1903301.
(37) Xu, C.-H.; Ye, P.-J.; Zhou, Y.-C.; He, D.-X.; Wei, H.; Yu, C.-Y. Cell membrane-camouflaged nanoparticles as drug carriers for cancer therapy. *Acta Biomater.* **2020**, *105*, 1−14.
(38) Ochyl, L. J.; Moon, J. J. Dendritic Cell Membrane Vesicles for Activation and Maintenance of Antigen-Specific T Cells. *Adv. Healthcare Mater.* **2019**, *8*, No. e1801091.
(39) Kovar, M.; Boyman, O.; Shen, X.; Hwang, I.; Kohler, R.; Sprent, J. Direct stimulation of T cells by membrane vesicles from antigen-presenting cells. *Proc. Natl. Acad. Sci. U. S. A.* **2006**, *103*, 11671−11676.
(40) Sprent, J. Direct stimulation of naïve T cells by antigen-presenting cell vesicles. *Blood Cells Mol., Dis.* **2005**, *35*, 17−20.
(41) Théry, C.; Duban, L.; Segura, E.; Véron, P.; Lantz, O.; Amigorena, S. Indirect activation of naïve CD4+ T cells by dendritic cell−derived exosomes. *Nat. Immunol.* **2002**, *3*, 1156−1162.
(42) Neupane, K. R.; McCorkle, J. R.; Kopper, T. J.; Lakes, J. E.; Aryal, S. P.; Abdullah, M.; Snell, A. A.; Gensel, J. C.; Kolesar, J.; Richards, C. I. Macrophage-Engineered Vesicles for Therapeutic Delivery and Bidirectional Reprogramming of Immune Cell Polarization. *ACS Omega* **2021**, *6*, 3847−3857.
(43) Zhou, M.; Philips, M. R. Nitrogen Cavitation and Differential Centrifugation Allows for Monitoring the Distribution of Peripheral Membrane Proteins in Cultured Cells. *JoVE* **2017**, *126*, No. e56037.
(44) Burden, D. W. Guide to the disruption of biological samples - 2012. *Random Primers* **2012**, *12*, 1−25.
(45) Snell, A. A.; Neupane, K. R.; McCorkle, J. R.; Fu, X.; Moonschi, F. H.; Caudill, E. B.; Kolesar, J.; Richards, C. I. Cell-Derived Vesicles for in Vitro and in Vivo Targeted Therapeutic Delivery. *ACS Omega* **2019**, *4*, 12657−12664.
(46) Benvenuti, F.; Lagaudrière-Gesbert, C.; Grandjean, I.; Jancic, C.; Hivroz, C.; Trautmann, A.; Lantz, O.; Amigorena, S. Dendritic cell maturation controls adhesion, synapse formation, and the duration of the interactions with naive T lymphocytes. *J. Immunol.* **2004**, *172*, 292−301.
(47) Mbongue, J. C.; Nieves, H. A.; Torrez, T. W.; Langridge, W. H. R. The Role of Dendritic Cell Maturation in the Induction of Insulin-Dependent Diabetes Mellitus. *Front. Immunol.* **2017**, *8*, 327.
(48) Alloatti, A.; Kotsias, F.; Magalhaes, J. G.; Amigorena, S. Dendritic cell maturation and cross-presentation: timing matters! *Immunol. Rev.* **2016**, *272*, 97−108.
(49) Verdijk, P.; van Veelen, P. A.; de Ru, A. H.; Hensbergen, P. J.; Mizuno, K.; Koerten, H. K.; Koning, F.; Tensen, C. P.; Mommaas, A. M. Morphological changes during dendritic cell maturation correlate with cofilin activation and translocation to the cell membrane. *Eur. J. Immunol.* **2004**, *34*, 156−164.
(50) Kim, M. K.; Kim, J. Properties of immature and mature dendritic cells: phenotype, morphology, phagocytosis, and migration. *RSC Adv.* **2019**, *9*, 11230−11238.
(51) Segura, E.; Nicco, C.; Lombard, B.; Véron, P.; Raposo, G.; Batteux, F.; Amigorena, S.; Théry, C. ICAM-1 on exosomes from mature dendritic cells is critical for efficient naive T-cell priming. *Blood* **2005**, *106*, 216−223.
(52) Yamakita, Y.; Matsumura, F.; Lipscomb, M. W.; Chou, P. C.; Werlen, G.; Burkhardt, J. K.; Yamashiro, S. Fascin1 promotes cell migration of mature dendritic cells. *J. Immunol.* **2011**, *186*, 2850−2859.
(53) Chernyshev, V. S.; Rachamadugu, R.; Tseng, Y. H.; Belnap, D. M.; Jia, Y.; Branch, K. J.; Butterfield, A. E.; Pease, L. F., III; Bernard, P. S.; Skliar, M. Size and shape characterization of hydrated and desiccated exosomes. *Anal. Bioanal. Chem.* **2015**, *407*, 3285−3301.
(54) Chuo, S. T.-Y.; Chien, J. C.-Y.; Lai, C. P.-K. Imaging extracellular vesicles: current and emerging methods. *J. Biomed. Sci. Eng.* **2018**, *25*, 91.
(55) Wu, Y.; Deng, W.; Klinke, D. J., II Exosomes: improved methods to characterize their morphology, RNA content, and surface protein biomarkers. *Analyst* **2015**, *140*, 6631−6642.

https://doi.org/10.1021/acsomega.2c04420
ACS Omega 2022, 7, 46222−46233

(56) González-Amaro, R.; Cortés, J. R.; Sánchez-Madrid, F.; Martín, P. Is CD69 an effective brake to control inflammatory diseases? *Trends Mol. Med.* **2013**, *19*, 625.
(57) Hood, J. L. The association of exosomes with lymph nodes. *Semin. Cell Dev. Biol.* **2017**, *67*, 29−38.
(58) Kirchhausen, T.; Macia, E.; Pelish, H. E. Use of Dynasore, the Small Molecule Inhibitor of Dynamin, in the Regulation of Endocytosis. In *Methods in Enzymology*; Vol. *438*; Academic Press, 2008; pp. 77−93.

https://doi.org/10.1021/acsomega.2c04420
ACS Omega 2022, 7, 46222−46233